

Shear-Induced Isotropic-to-Nematic Transition in a Thermotropic Liquid-Crystalline Polymer

Chang Dae Han* and Seung Su Kim†

Department of Polymer Engineering, The University of Akron, Akron, Ohio 44325-0301

Received September 30, 1994

Revised Manuscript Received January 9, 1995

Introduction

Over the last two decades, flow-induced phase transition in polymer systems has been an active research area. Specifically, flow-induced crystallization in polymer solutions or melts has been extensively discussed, and readers are referred to a research monograph edited by Miller,¹ summarizing the research activities in the 1970s, and a series of more recent papers by McHugh and co-workers² and references therein. There is a general agreement among researchers that crystallization is facilitated when a polymer solution or melt is subjected to a flow field. However, regarding the effect of a flow field on phase transition in mixtures of polymer and solvent or in mixtures of two polymers in either the solution or molten state, there are two opposing experimental observations reported in the literature. Specifically, some research groups^{3–5} presented experimental evidence that application of shearing promoted phase separation (i.e., shear-induced demixing effect), which is predicted by theory.^{6,7} On the other hand, other research groups^{8–12} presented experimental evidence that a homogenization (i.e., flow-induced mixing effect) is facilitated when a two-phase mixture of polymers is subjected to a shear flow field. It should be mentioned that in some cases a phase transition was noted after cessation of shearing.^{3,8}

In recent years, liquid-crystalline polymers (LCPs) have attracted the attention of polymer scientists, and the flow-induced isotropic-to-anisotropic phase transition in an LCP has been studied theoretically.^{13–16} Specifically, Marrucci and Ciferri¹³ have shown that an elongational flow can induce a transition to the nematic phase at a concentration below that predicted by the Flory theory¹⁷ of rodlike molecules in the absence of a flow field. Thirumalai¹⁵ considered the same problem using the Onsager expression¹⁸ for the excess energy and performed numerical calculations to construct plots of the free energy difference between the isotropic phase and the nematic phase as a function of concentration. He concluded that the ordered nematic phase is more stable than the disordered isotropic phase. See et al.¹⁶ considered the stability of steady-state solutions of the Doi kinetic equation¹⁹ for rigid-rodlike polymer solutions in an arbitrary flow field and predicted that for a certain range of concentrations, the isotropic-to-nematic (I–N) transition can be induced by imposing a flow, if the flow rate exceeds a certain critical value and the critical flow rate decreases as concentration is increased.

However, to the best of our knowledge, there is no experimental study which has investigated the onset of the I–N transition in a thermotropic LCP. The scarcity of such studies is believed to be due to the fact that the majority of the thermotropic LCPs synthesized have relatively high clearing (or isotropization) temperatures

(T_{NI}). For instance, the two well-known commercially available thermotropic LCPs, copolyesters of *p*-hydroxybenzoic acid (HBA) and poly(ethylene terephthalate) (PET) and copolyesters of HBA and 6-hydroxy-2-naphthoic acid (HNA), are reported to have T_{NIS} above 400 °C, which is close to their thermal degradation temperatures. Using such polymers, it is virtually impossible to investigate the onset of a shear-induced I–N transition.

Recently, using a cone-and-plate rheometer, we observed evidence of a shear-induced I–N transition in a thermotropic LCP, poly[(phenylsulfonyl)-*p*-phenylene 1,10-decamethylenebis(4-oxybenzoate)] (PSHQ10), which was synthesized in our laboratory. We reported earlier that PSHQ10 has a melting temperature of 115 °C and a T_{NI} of 175 °C as determined by differential scanning calorimetry (DSC).²⁰ PSHQ10 has several unique features which have allowed us to observe the shear-induced I–N phase transition: (a) PSHQ10 has a well-defined nematic structure (schlieren textures), as determined from cross-polarized optical microscopy,^{20,21} at temperatures ranging from about 115 to about 175 °C, and (b) it enables us to completely erase any previous thermal histories associated with polymerization and sample preparation, by first heating a specimen to an isotropic state (e.g., 190 °C) and then shearing there at a low shear rate for about 4–5 min, before being cooled to a predetermined temperature above its T_{NI} (175 °C).²⁰ In this paper we report the highlights of our findings.

Experimental Section

The details of the synthesis procedures for PSHQ10 are given in previous papers.^{22,23} In the present study, rheological measurements were conducted to observe the shear-induced I–N transition. For the study, specimens for rheological measurements were prepared by first dissolving PSHQ10 in dichloromethane in the presence of an antioxidant (Irganox 1010, Ciba-Geigy Group) and then slowly evaporating the solvent at room temperature for a week. The cast films with the thickness of 1 mm were further dried in a vacuum oven at room temperature for at least 3 weeks and at 90 °C for 48 h. Right before rheological measurement, the specimen was further dried at 120 °C for 2 h to remove any residual solvent and moisture.

For rheological measurements, a Model R16 Weissenberg rheogoniometer (Sangamo Control, Inc.) in the cone-and-plate (25 mm diameter plate and 4° cone angle) configuration was used to measure (a) in the steady-state shear mode, the shear stress (σ) and first normal stress difference (N_1) as functions of shear rate ($\dot{\gamma}$), and (b) in the oscillatory shear mode, the dynamic storage and loss moduli (G' and G'') as functions of angular frequency (ω) under isothermal conditions. From the measurements of G' and G'' , the absolute value of the complex viscosity $|\eta^*(\omega)|$ was calculated using the relationship $|\eta^*(\omega)| = [(G'(\omega)/\omega)^2 + (G''(\omega)/\omega)^2]^{1/2}$. Strain amplitude was varied from 0.01 to 0.06, which was well within the linear viscoelastic range of the materials investigated. This, together with data acquisition during measurement, was accomplished with the aid of a microcomputer interfaced with the rheometer. All experiments were conducted in the presence of nitrogen to preclude oxidative degradation of the specimen. Temperature control was satisfactory to within ± 1 °C.

The experimental procedure employed in the present study is as follows. An as-cast specimen was first heated to 190 °C for 5 min, while being sheared there at a rate of 0.008 s⁻¹, and then slowly cooled to a predetermined temperature (176, 177, or 180 °C), which is still above the T_{NI} (175 °C) of PSHQ10. We then employed the following experimental protocols: (1) A shear flow at a predetermined shear rate was applied to the specimen for a fixed period. (2) After cessation of shear

* Present address: Research and Development Center, Miwon Petrochemical Corp., Ulsan 780-140, Republic of Korea.

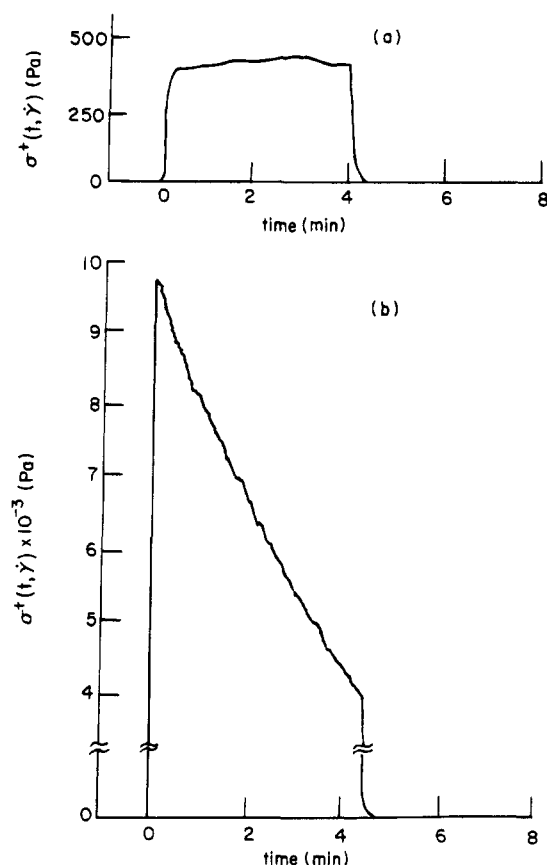


Figure 1. Trace of transient shear stress $\sigma^+(t, \dot{\gamma})$ for a PSHQ10 specimen at 176 °C: (a) at $\dot{\gamma} = 0.02 \text{ s}^{-1}$; (b) at $\dot{\gamma} = 0.54 \text{ s}^{-1}$.

flow, small-amplitude oscillatory deformations (strain $\gamma_0 = 0.02$ and angular frequency $\omega = 0.075 \text{ rad/s}$) were applied to the specimen, and values of G' , G'' , and $|\eta^*|$ were recorded during the rest period. It is well established that for *isotropic* fluids, values of G' , G'' , and $|\eta^*|$ remain constant after cessation of shear flow. It should be mentioned that earlier some investigators²⁴⁻²⁷ used the time evolution of G' , G'' , or $|\eta^*|$ as a means of monitoring "structural recovery" for lyotropic or thermotropic LCPs after being subjected to a shear flow. The rationale behind such an approach lies in that the dynamic viscoelastic properties have been found to be very sensitive to the microstructure of polymers, in particular LCPs, whose morphologies are very much affected by both thermal and deformation histories.

Results and Discussion

The first experimental evidence that we observed in this study of shear-induced I–N transition in a PSHQ10 specimen at 176 °C, which is slightly above the T_{NI} , is displayed in Figure 1, where the traces of transient shear stress $\sigma^+(t, \dot{\gamma})$ at $\dot{\gamma} = 0.02$ and 0.54 s^{-1} , respectively, are given. It can be seen in Figure 1 that at $\dot{\gamma} = 0.54 \text{ s}^{-1}$ the shear stress initially goes through a large overshoot and then steadily decreases with time, whereas at $\dot{\gamma} = 0.02 \text{ s}^{-1}$ there is *no* overshoot in shear stress. When a shear flow at $\dot{\gamma} = 0.54 \text{ s}^{-1}$ was applied to a PSHQ10 specimen at 190 °C, we did *not* observe any overshoot in shear stress, and shear stress remained constant during shearing. Note that the steady decrease in shear stress after an overshoot, given in Figure 1b, indicates that shear viscosity decreases during shearing. This can be regarded as being evidence of the shear-induced I–N transition, because it is well documented in the literature²⁸⁻³² that the viscosity of an anisotropic phase is lower than that of the isotropic phase; i.e., under shear flow the nematic phase of

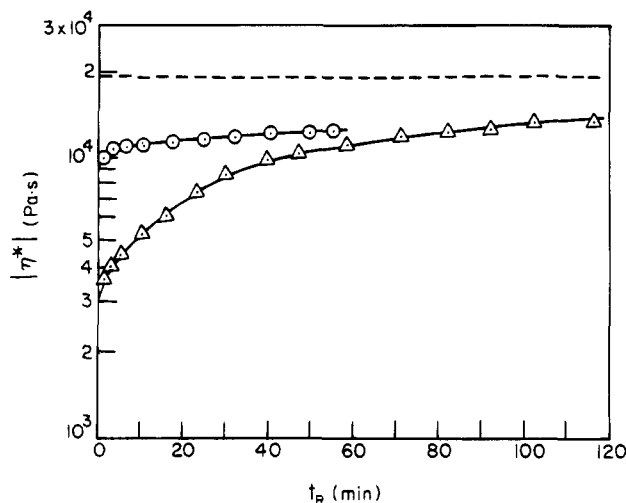


Figure 2. Time evolution of $|\eta^*|$ for PSHQ10 specimens at 177 °C under small-amplitude oscillatory deformations after the specimen had been subjected to steady shear flow at $\dot{\gamma} = 0.43 \text{ s}^{-1}$ for 36 min (\circ) and at $\dot{\gamma} = 0.68 \text{ s}^{-1}$ for 57 min (Δ). The dashed horizontal line represents the value of $|\eta^*|$ for a specimen before being subjected to steady shear flow.

PSHQ10 orients along the shear direction and thus the viscosity of the nematic phase is expected to be lower than that of the isotropic phase. Below we shall show, using $\log G'$ versus $\log G''$ plots, that the PSHQ10 specimen at 176 °C, before being subjected to shear flow, was at the isotropic state. It should be mentioned that the trace of $\sigma^+(t, \dot{\gamma})$ given in Figure 1b was reproducible when using other fresh specimens. We observed, however, that the trace of $\sigma^+(t, \dot{\gamma})$ for PSHQ10 at 176 °C during shearing at $\dot{\gamma} > 0.85 \text{ s}^{-1}$ exhibited very irregular patterns and, moreover, was *not* reproducible. Under such situations, we found that the meniscus of the specimen was broken, indicating that a hydrodynamic instability had set in during the transient shear flow.

We will now present other evidence that we observed in this study of the shear-induced I–N phase transition in PSHQ10. Figure 2 gives variations of $|\eta^*|$ with rest time t_R for PSHQ10 at 177 °C after being sheared at $\dot{\gamma} = 0.43$ and 0.68 s^{-1} , respectively, until steady state was reached. Note that the dashed line in Figure 2 denotes the value of $|\eta^*|$ just before the specimen was subjected to a steady shear flow and, thus, the dashed line represents the melt in an *isotropic* state. It can be seen in Figure 2 that the value of $|\eta^*|$ increased very slowly when the specimen was sheared at $\dot{\gamma} = 0.43 \text{ s}^{-1}$, as compared to the situation where the specimen was sheared at $\dot{\gamma} = 0.68 \text{ s}^{-1}$. Notice in Figure 2 that the higher the shear rate during shear flow, the lower the initial value $|\eta^*|_i$ upon cessation of shear flow and that the difference between the initial value $|\eta^*|_i$ and the final value $|\eta^*|_f$ became greater as the shear rate increased. What is apparent in Figure 2 is that the rate of increase in $|\eta^*|$ with t_R is greater with increasing shear rate, which was applied to the specimen during shear flow, approaching the value of $|\eta^*|$ for an *isotropic* state (denoted by a dashed line). It should be mentioned that there was *no* change in $|\eta^*|$ when the applied shear rate was very low.

In order to ascertain whether or not the I–N transition may be induced by applying shear flow, we made another very interesting rheological observation, namely, the time evolution of the logarithmic plot of G' versus G'' during the rest period. Figure 3 gives the time evolution of $\log G'$ versus $\log G''$ plot for a PSHQ10

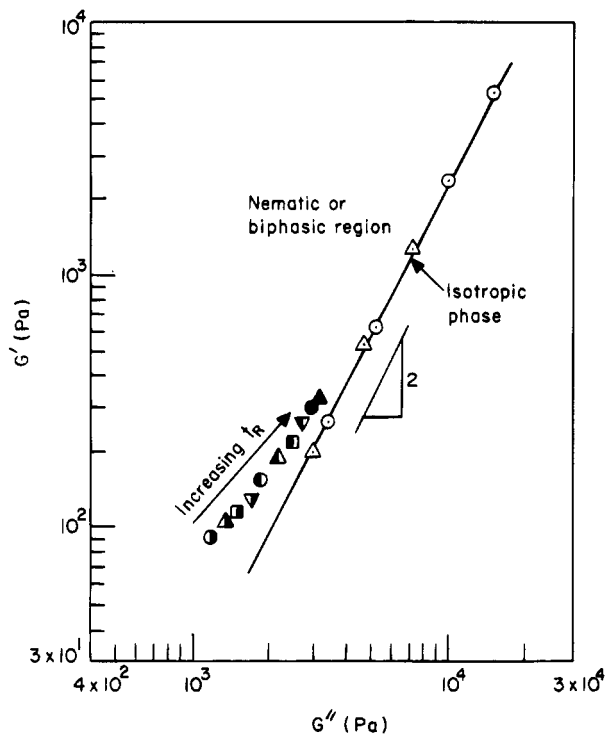


Figure 3. Plots of $\log G'$ versus $\log G''$ for a PSHQ10 specimen: (○) at 190 °C; (Δ) at 176 °C before being subjected to shear flow. Other symbols: during the rest period of (○) 1, (Δ) 3, (□) 6, (▽) 11, (◇) 18, (Δ) 30, (□) 46, (▽) 65, (◇) 80, and (Δ) 140 min after the specimen at 176 °C had been subjected to shear flow at $\dot{\gamma} = 0.34 \text{ s}^{-1}$ for 17 min 25 s.

specimen at 176 °C after cessation of shear flow at $\dot{\gamma} = 0.34 \text{ s}^{-1}$ for 17 min 25 s. Similar plots are given in Figure 4 for a PSHQ10 specimen at 176 °C after cessation of shear flow at $\dot{\gamma} = 0.85 \text{ s}^{-1}$ for 7 min. Also given in Figures 3 and 4 are, for comparison, plots of $\log G'$ versus $\log G''$ for the PSHQ10 specimens which were prepared from the oscillatory shear flow data taken in an *isotropic* state at 190 °C (○) and at 176 °C before the specimen had been subjected to a shear flow (Δ). The fact that $\log G'$ versus $\log G''$ plots for PSHQ10 specimens, before being subjected to shear flow, lie on the same correlations having the slope of 2 at both 176 and 190 °C attests that the PSHQ10 specimen at 176 °C, which gave rise to the transient shear stresses given in Figure 1b, was indeed at the *isotropic* state before being subjected to shear flow.

Note in Figures 3 and 4 that each data point (partially and fully filled symbols) was taken at different rest times. It is of interest to observe in Figures 3 and 4 that the $\log G'$ versus $\log G''$ plot *after* cessation of shear flow approaches that in the *isotropic* state and that the larger the applied shear rate, the faster the *anisotropic* state approaches the *isotropic* state during the rest period. This observation leads us to conclude that a PSHQ10 specimen at 176 °C, when sheared at $\dot{\gamma} = 0.34$ or 0.85 s^{-1} , was driven to a *nematic* region and that as t_R increases, the specimen driven to a *nematic* state tends to return to an *isotropic* state; i.e., *reverse* phase transition takes place after cessation of shear flow. This interpretation is based on the earlier experimental observations^{33–39} that for flexible homopolymers $\log G'$ versus $\log G''$ plots in the terminal region, having a slope of 2, are virtually independent of temperature and that $\log G'$ versus $\log G''$ plots for microphase-separated block copolymers at temperatures below a certain critical value (often referred to as the order–disorder

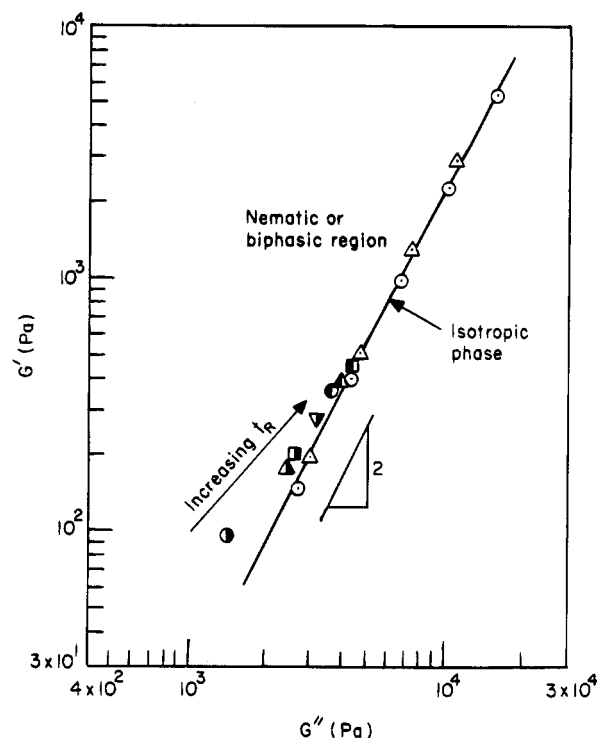


Figure 4. Plots of $\log G'$ versus $\log G''$ for PSHQ10 specimen: (○) at 190 °C; (Δ) at 176 °C before being subjected to shear flow. Other symbols: during the rest period of (○) 11, (Δ) 13, (□) 16, (▽) 22, (◇) 31, (Δ) 40, and (□) 77 min after the specimen at 176 °C had been subjected to shear flow at $\dot{\gamma} = 0.85 \text{ s}^{-1}$ for 7 min.

transition temperature T_{ODT}) vary with temperature but are virtually independent of temperature at temperatures $T \geq T_{ODT}$. Han and co-workers^{37–39} observed further that $\log G'$ versus $\log G''$ plots for a block copolymer in the *ordered* (microphase-separated) state lie on the left side of the $\log G'$ versus $\log G''$ plot in the *disordered* (homogeneous) state and that as the temperature of the block copolymer increased toward its T_{ODT} , its $\log G'$ versus $\log G''$ plot approached the $\log G'$ versus $\log G''$ plot in the *disordered* state. We hasten to add, in reference to Figures 3 and 4, that when the applied shear rates were very low (say, $\dot{\gamma} < 0.1 \text{ s}^{-1}$), the $\log G'$ versus $\log G''$ plot was found to lie on the curve representing the *isotropic* state. We thus conclude from Figures 3 and 4 that the *nematic* phase was induced when the shear rate applied to the *isotropic* phase of PSHQ10 exceeded a certain *critical* value.

Concluding Remarks

In this paper we have presented experimental evidence from rheological measurements that the I–N transition was induced at a critical shear rate in a thermotropic liquid-crystalline polyester (PSHQ10) that we synthesized in our laboratory. This study was made possible by the fact that PSHQ10 has a relatively low T_{NI} (which is ca. 175 °C as determined by DSC under quiescent conditions), enabling us to raise the experimental temperature, without having thermal degradation of the material, to an *isotropic* state. In determining whether or not a specimen under shear flow was driven to a *nematic* state, after cessation of the steady shear flow we applied small-amplitude oscillatory shear deformations to the specimen and monitored the time evolution of G' , G'' , and $|\eta^*|$. Using the $\log G'$ versus $\log G''$ plots, we found that the reverse (i.e., from *nematic* to *isotropic*) phase transition was taking place

during the rest period. We believe that this rheological method would be equally applicable to other types of thermotropic LCPs. We learned that there are three variables that influence the shear-induced I–N transition of a thermotropic LCP; they are (a) shear rate, (b) duration of shearing (or shear strain), and (c) temperature. These variables are interrelated, insofar as determining the conditions for the onset of the shear-induced I–N transition. We made an observation that when the temperature of a specimen is very close to its T_{NI} , a very low shear rate or a small shear strain is sufficient to induce the I–N phase transition, whereas when the temperature of a specimen is far above its T_{NI} , a very high shear rate or a very large shear strain is required to induce the I–N transition.

In the future, using a suitably designed apparatus we plan to make a direct visual observation, during shear flow on the formation of an *anisotropic* phase as the applied shear rate exceeds a certain critical value.

References and Notes

- (1) Miller, R. L., Ed. *Flow-Induced Crystallization in Polymer Systems*; Gordon and Breach: New York, 1979.
- (2) (a) McHugh, A. J.; Blank, R. H. *Macromolecules* **1986**, *19*, 1249. (b) McHugh, A. J.; Spevacek, J. A. *J. Polym. Sci., Part C: Polym. Lett.* **1987**, *25*, 105. (c) McHugh, A. J.; Spevacek, J. A. *J. Polym. Sci., Part B: Polym. Phys.* **1991**, *29*, 969.
- (3) Ver Strate, G.; Philippoff, W. *J. Polym. Sci., Polym. Lett. Ed.* **1974**, *12*, 267.
- (4) Rangel-Nafaile, C.; Metzner, A. B.; Wissbrun, K. F. *Macromolecules* **1984**, *17*, 1187.
- (5) Hammouda, B.; Nakatani, A. I.; Waldow, D. A.; Han, C. C. *Macromolecules* **1992**, *25*, 2903.
- (6) Onuki, A. *Phys. Rev. Lett.* **1989**, *62*, 2472.
- (7) Onuki, A. *J. Phys. Soc. Jpn.* **1990**, *59*, 3427.
- (8) Silverberg, A.; Kuhn, W. *J. Polym. Sci.* **1954**, *13*, 21.
- (9) (a) Mazich, K. A.; Carr, S. H. *J. Appl. Phys.* **1983**, *54*, 5511. (b) Rector, L. P.; Mazich, K. A.; Carr, S. H. *J. Macromol. Sci., Phys.* **1988**, *B24*, 421.
- (10) Katsaros, J. D.; Malone, M. F.; Winter, H. H. *Polym. Bull.* **1986**, *16*, 83.
- (11) Lyngaae-Jorgenson, J.; Sondergaard, K. *Polym. Eng. Sci.* **1987**, *27*, 344, 351.
- (12) Hindawi, I.; Higgins, J. S.; Galambos, A. F.; Weiss, R. A. *Macromolecules* **1990**, *23*, 670.
- (13) Marrucci, G.; Ciferri, A. *J. Polym. Sci., Polym. Lett. Ed.* **1977**, *15*, 643.
- (14) Marrucci, G.; Sarti, G. C. In *Ultra-High Modulus Polymers*; Ciferri, A., Ward, I. M., Eds.; Applied Science Publishers: London, 1979; Chapter 4.
- (15) Thirumalai, D. *J. Chem. Phys.* **1986**, *84*, 5869.
- (16) See, H.; Doi, M.; Larson, R. G. *J. Chem. Phys.* **1990**, *92*, 792.
- (17) Flory, P. J. *Proc. R. Soc. London* **1956**, *A234*, 60, 73.
- (18) Onsager, L. *Ann. N.Y. Acad. Sci.* **1949**, *51*, 627.
- (19) Doi, M. *J. Polym. Sci., Polym. Phys. Ed.* **1981**, *19*, 229.
- (20) Kim, S. S.; Han, C. D. *Macromolecules* **1993**, *26*, 3176.
- (21) Rojstaczer, S. R.; Stein, R. S. *Macromolecules* **1990**, *23*, 4863.
- (22) Furukawa, A.; Lenz, R. W. *Makromol. Chem., Macromol. Symp.* **1986**, *2*, 3.
- (23) Kim, S. S.; Han, C. D. *Polymer* **1994**, *35*, 93.
- (24) Moldenaers, P.; Mewis, J. *J. Rheol.* **1986**, *30*, 567.
- (25) Mewis, J.; Moldenaers, P. *Chem. Eng. Commun.* **1987**, *53*, 33.
- (26) Grizzuti, N.; Cavella, S.; Cicarelli, P. *J. Rheol.* **1990**, *34*, 1293.
- (27) Guskey, S. M.; Winter, H. H. *J. Rheol.* **1991**, *35*, 1191.
- (28) Hermans, J. *J. Colloid Sci.* **1962**, *17*, 638.
- (29) Papkov, S. P.; Kulichikhin, B. G.; Kalmykovam, V. D.; Malkin, A. Ya. *J. Polym. Sci., Polym. Phys. Ed.* **1974**, *12*, 1753.
- (30) Kiss, G.; Porter, R. S. *J. Polym. Sci., Polym. Symp.* **1978**, *65*, 193.
- (31) Wunder, S. L.; Ramachandran, S.; Gochanour, S. R.; Weinberg, M. *Macromolecules* **1986**, *19*, 1696.
- (32) Gonzalez, J. M.; Munoz, M. E.; Cortazar, M.; Santamaria, A.; Pena, J. J. *J. Polym. Sci., Polym. Phys. Ed.* **1990**, *28*, 1533.
- (33) Han, C. D.; Lem, K. W. *Polym. Eng. Rev.* **1983**, *2*, 135.
- (34) Han, C. D.; Chuang, H. K. *J. Appl. Polym. Sci.* **1985**, *30*, 2431.
- (35) Han, C. D.; Jhon, M. S. *J. Appl. Polym. Sci.* **1986**, *32*, 3809.
- (36) Han, C. D. *J. Appl. Polym. Sci.* **1988**, *35*, 167.
- (37) Han, C. D.; Kim, J. *J. Polym. Sci., Part B: Polym. Phys.* **1987**, *25*, 1741.
- (38) Han, C. D.; Kim, J.; Kim, J. K. *Macromolecules* **1989**, *22*, 383.
- (39) Han, C. D.; Baek, D. M.; Kim, J. K. *Macromolecules* **1990**, *23*, 561.

MA945077K